Chemical Engineering Journal 155 (2009) 396–403

Contents lists available at ScienceDirect

Chemical Engineering Journal

journal homepage: www.elsevier.com/locate/cej

Ethylene epoxidation in low-temperature AC corona discharge over Ag catalyst: Effect of promoter

Thammanoon Sreethawong[a,b], Thanapoom Suwannabart[a], Sumaeth Chavadej[a,b,*]

[a] The Petroleum and Petrochemical College, Chulalongkorn University, Soi Chula 12, Phyathai Road, Pathumwan, Bangkok 10330, Thailand
[b] Center for Petroleum, Petrochemicals, and Advanced Materials, Chulalongkorn University, Bangkok 10330, Thailand

ARTICLE INFO

Article history:
Received 19 May 2009
Received in revised form 29 July 2009
Accepted 31 July 2009

Keywords:
Epoxidation
Ethylene oxide
Corona discharge
Ag catalyst
Promoter

ABSTRACT

In this work, the epoxidation of ethylene using a low-temperature corona discharge system was investigated with various reported catalytically active catalysts: Ag/α-Al_2O_3, Cs–Ag/α-Al_2O_3, Cu–Ag/α-Al_2O_3, and Au–Ag/α-Al_2O_3. It was experimentally found that the investigated catalysts could improve the ethylene conversion and the ethylene oxide (EO) yield and selectivity for the corona discharge system, particularly 1 wt.% Cs–12.5 wt.% Ag/α-Al_2O_3 and 0.2 wt.% Au–12.5 wt.% Ag/α-Al_2O_3. The power consumption per EO molecule produced in the corona discharge system, combined with the superior bimetallic catalysts, was much lower than that of the sole corona discharge system and that of the corona discharge system combined with the monometallic Ag catalyst.

1. Introduction

Ethylene epoxidation is an important process in the petrochemical industry for producing a versatile ethylene oxide (C_2H_4O, EO) molecule. The most widely used technique for ethylene oxide production is catalytic processes using silver-based catalysts. Silver catalysts supported on low-surface area α-alumina (Ag/(LSA)α-Al_2O_3) provide high EO selectivity [1–4]. Some previous research has revealed that alkali and transition metals, especially cesium (Cs) [5–11], copper (Cu) [12–15], and gold (Au) [16–21], also provide the improvement of the EO selectivity. However, the conventional catalytic processes are generally facilitated by a high temperature operation, implying high energy consumption. The normal temperature used for such processes is at least 200 °C. In addition, the use of high temperatures for ethylene epoxidation inevitably causes operational problems, i.e., catalyst deactivation, catalyst regeneration, and catalyst replacement. To develop and apply a new low-temperature plasma technique for ethylene epoxidation would be attractive for lowering the energy consumption and alleviating the catalytic problems.

Non-thermal plasma is considered to be an interesting potential replacement for the conventional catalytic processes for ethylene epoxidation. It is one kind of electric gas discharge, in which electrons gain enough energy from an external applied voltage to overcome the potential barrier of metal surface electrodes [22]. Subsequently, these energetic electrons can move from one electrode to the other and instantaneously collide with gaseous molecules in the plasma zone to generate highly active atoms, molecules, and radicals by excitation and dissociation reactions. The excited and dissociated species can rapidly bring about the formation of new chemical species. A great advantage of non-thermal plasma is that the generated electrons have a high temperature of approximately 10^4–10^5 K, while the bulk gas still has a much lower temperature, close to room temperature [23–25], leading to a lower energy requirement as compared to the conventional catalytic processes. Moreover, the low-temperature operation of non-thermal plasma is expected to enable its combined use with a catalyst, without the aforementioned catalytic problems.

In our previous work, ethylene epoxidation using a low-temperature corona discharge system was, for the first time, studied both in the absence and in the presence of various powder catalysts, including Ag/(LSA)α-Al_2O_3, Ag/(high-surface area, HSA)γ-Al_2O_3, Au–Ag/(HSA)γ-Al_2O_3, and Au/TiO_2 [26]. The results showed that the combination of corona discharge and the reported highly active Ag/(LSA)α-Al_2O_3 catalyst with an optimum Ag loading of 12.5 wt.% offered the highest EO selectivity. Furthermore, ethylene epoxidation was investigated using a low-temperature dielectric barrier discharge (DBD) system [27]. Because the large-surface area parallel plate electrodes of the DBD reactor (as compared to that of the pin and circular plate electrodes of corona discharge reactors) led to a difficulty in packing the powder catalysts between them, the DBD system was only operated without

* Corresponding author at: The Petroleum and Petrochemical College, Chulalongkorn University, Soi Chula 12, Phyathai Road, Pathumwan, Bangkok 10330, Thailand. Tel.: +66 2 218 4139; fax: +66 2 218 4139.
E-mail address: sumaeth.c@chula.ac.th (S. Chavadej).

1385-8947/$ – see front matter © 2009 Elsevier B.V. All rights reserved.
doi:10.1016/j.cej.2009.07.056

catalysts. However, it can be concluded from the experimental results of the previous work that both low-temperature corona discharge and DBD systems are highly potential candidates to be used for ethylene epoxidation. In this extended work, the effect of promoter (Cs, Cu, and Au) on the ethylene epoxidation activity over a 12.5 wt.% Ag/(LSA)α-Al_2O_3 catalyst using a low-temperature corona discharge system was investigated.

2. Experimental

2.1. Materials and reactant gases

In this work, the support used was (LSA)α-Al_2O_3 (A.C.S. Xenon). Silver nitrate ($AgNO_3$, Carlo Erba), cesium nitrate ($CsNO_3$, Merck), copper nitrate trihydrate ($Cu(NO_3)_2{\cdot}3H_2O$, Merck), and hydrogen tetrachloroaurate trihydrate ($HAuCl_4{\cdot}3H_2O$, Alfa Aesar) were employed as silver, cesium, copper, and gold catalyst precursors, respectively. All chemicals were used as received without further purification. For the reactant gases, 99.995% helium (high purity grade), 40% ethylene balanced with helium, and 97% oxygen balanced with helium were used and were supplied by Thai Industrial Gas (Public) Co., Ltd.

2.2. Catalyst preparation procedure

All bimetallic catalysts were prepared by the sequential incipient wetness impregnation method using (LSA)α-Al_2O_3 as the catalyst support. First, a Ag catalyst on the (LSA)α-Al_2O_3 support was prepared by using a $AgNO_3$ aqueous solution at a nominal loading of 12.5 wt.% Ag, which was found to provide the maximum EO selectivity with relatively high ethylene and oxygen conversions [26]. After the mixture had been dried at 110 °C for 2 h, it was sequentially impregnated with an appropriate amount of a Cs, Cu, or Au promoter by using an aqueous solution of $CsNO_3$, $Cu(NO_3)_2{\cdot}3H_2O$, or $HAuCl_4{\cdot}3H_2O$. For each bimetallic catalyst, i.e., Cs–Ag/(LSA)α-Al_2O_3, Cu–Ag/(LSA)α-Al_2O_3, and Au–Ag/(LSA)α-Al_2O_3, the loadings of Cs, Cu, or Au were 0.2 and 1 wt.% for each. After that, these impregnated catalysts were dried in air at 110 °C overnight and then calcined in air at 400 °C for 12 h. Finally, all the prepared catalysts were sieved in order to obtain the desired grain size range of 221–425 μm for the reaction activity experiments.

2.3. Catalyst characterization techniques

The specific surface areas of all prepared catalysts were determined by a surface area analyzer (Quantachrom, Autosorb-1) using nitrogen adsorption analysis. A catalyst sample was dried and outgassed under vacuum at 150 °C for 10 h to remove the humidity and any volatile components adsorbed on the catalyst surface before the analysis. The crystalline phases of the prepared catalysts were investigated by an X-ray diffractometer (XRD, Rigaku RINT-2200) equipped with a graphite monochromator, a Cu tube for generating CuKα radiation (λ = 1.5406 Å) at a voltage of 40 kV and a current of 30 mA, and a nickel filter used as the filter for Kβ removal. The catalyst sample was examined in the 2θ range of 30–60° at a scan-

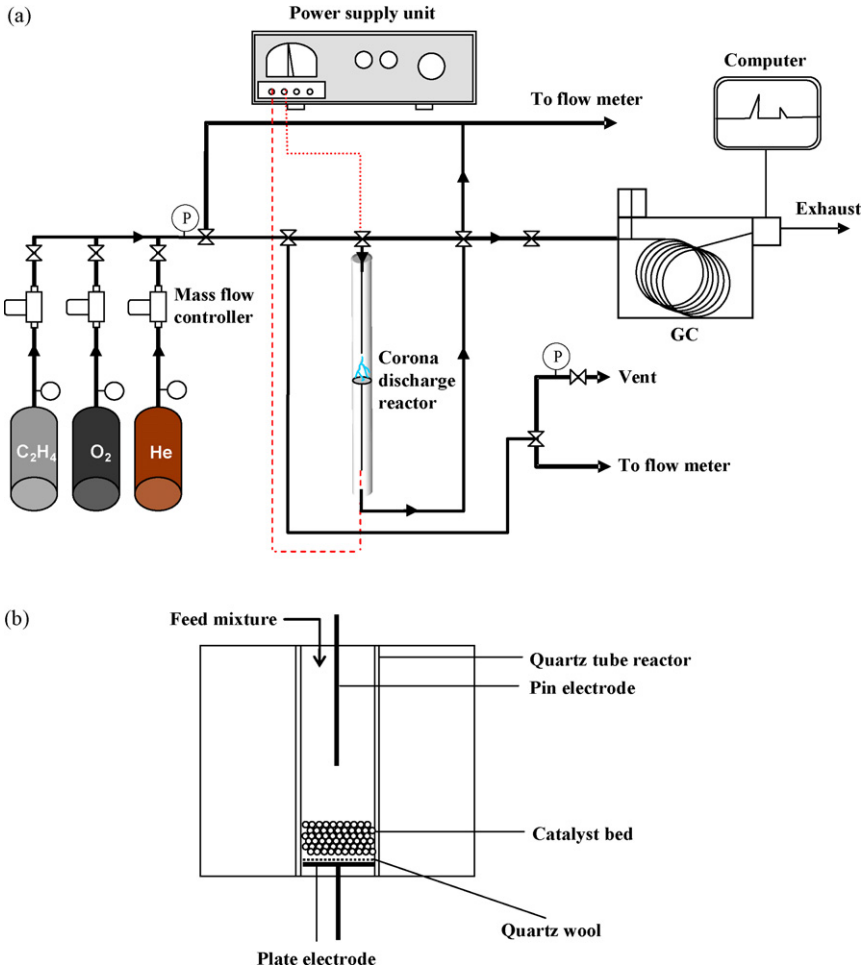

Fig. 1. (a) Schematic of experimental setup of corona discharge system and (b) configuration of the corona discharge reactor.

ning speed of 5°(2θ)/min. Transmission electron microscopy (TEM, JEOL 2000 CX) was employed for investigating the average particle size of the Ag particles on the prepared catalysts. The catalyst sample was ground into a fine powder and ultrasonically dispersed in ethanol. A small droplet of the suspension was placed on a copper grid, and the solvent was evaporated prior to loading the sample into the TEM. The TEM was operated at an accelerating voltage of 200 kV. Temperature-programmed oxidation (TPO) was employed to quantitatively investigate the coke deposition on the spent catalysts. The TPO analysis was performed at a continuous flow of O_2/He (ratio 2:1) with a total flow rate of 40 cm^3/min. A spent catalyst was placed in the quartz tube and was secured with packing quartz wool. The sample temperature was linearly increased to reach a maximum temperature of 850 °C in order to completely oxidize the carbon fraction of the deposited coke to CO_2. The effluent gas was passed through a methanator containing a Ni/Al_2O_3 catalyst to convert the CO_2 to methane at 400 °C. Subsequently, the produced methane was detected with a flame ionization detector (FID, SRI model 110). The area under the obtained curve was used to calculate the carbon content in the spent catalyst sample. In addition, the amount of coke deposited on the catalyst surface was also confirmed by the weight change of spent catalyst after the TPO analysis.

2.4. Reaction testing experiments

The ethylene epoxidation experiments were conducted in a corona discharge system, which was operated at ambient temperature and atmospheric pressure. The schematic of experimental setup of the corona discharge system and the configuration of the corona discharge reactor are shown in Fig. 1. The input power used to generate plasma was alternating current (AC) power, 200 V and 50 Hz, which was transmitted to a high voltage current via a power supply unit. The output voltage was adjusted by a function generator, whereas the sinusoidal wave signal was controlled and monitored by an oscilloscope. A quantity of 0.24 g of each studied catalyst was individually placed on the plate electrode and secured by a quartz wool layer. The base reaction conditions used for the comparative investigation were an O_2/C_2H_4 molar ratio of 1/1, a total feed gas flow rate of 50 cm^3/min, an applied voltage of 19 kV, an input frequency of 500 Hz, and an electrode gap distance of 10 mm. The flow rates of reactant gases (ethylene, oxygen, and helium) fed through the plasma reactor were controlled by a set of electronic mass flow controllers and transducers, supplied by SIERRA® Instrument Inc. A 7-μm in-line filter was placed upstream of each mass flow controller in order to trap any solid particles. A check valve was placed downstream of each mass flow controller to prevent any back flow of the reactant gases. All of the reactant gases were mixed inside a single line before being introduced into the plasma reactor. Prior to the reaction start-up, the feed gas mixture was first introduced into the plasma system without turning on the power supply unit. After the composition of outlet gas was invariant with time, it was turned on. The outlet of the reactor was either vented to the atmosphere via a rubber tube exhaust or was connected to an on-line gas chromatograph (GC, PerkinElmer, AutoSystem) for analysis of the product gases. The moisture in the product gas stream was removed by a water trap filter before entering a heated stainless steel line to the on-line GC. The GC was equipped with both a thermal conductivity detector (TCD) and an FID. For the TCD channel, a packed column (Carboxen 1000) was used for separating the product gases, which were H_2, O_2, CO, CO_2, and C_2H_4. For the FID channel, a capillary column (OV-Plot U) was used for the analysis of EO and other by-product gases, i.e., CH_4, C_2H_2, C_2H_6, and C_3H_8. However, there were some unknown products with small quantities produced during the reaction, which could not be analyzed. The composition of the product gas stream was determined by the GC every 20 min. After the system reached steady state, an analysis of the outlet gas composition was taken at least a few times. The experimental data taken under steady state conditions were averaged, and these averages were used to evaluate the performance of the plasma system.

To evaluate the process performance, the conversions of C_2H_4 and O_2 and the selectivities for products, including EO, CO, CO_2, H_2, CH_4, C_2H_2, C_2H_6, and traces of C_3, were considered. The conversion of either C_2H_4 or O_2 is defined as:

$$\%\text{reactant conversion} = \frac{(\text{moles of reactant in} - \text{moles of reactant out})(100)}{(\text{moles of reactant in})}$$

The product selectivity is calculated from the following equation:

$$\%\text{product selectivity} = \frac{[(\text{number of C or H atom in product})\,(\text{moles of product produced})]\,(100)}{(\text{number of C or H atom in } C_2H_4)\,(\text{moles of } C_2H_4 \text{ converted})}$$

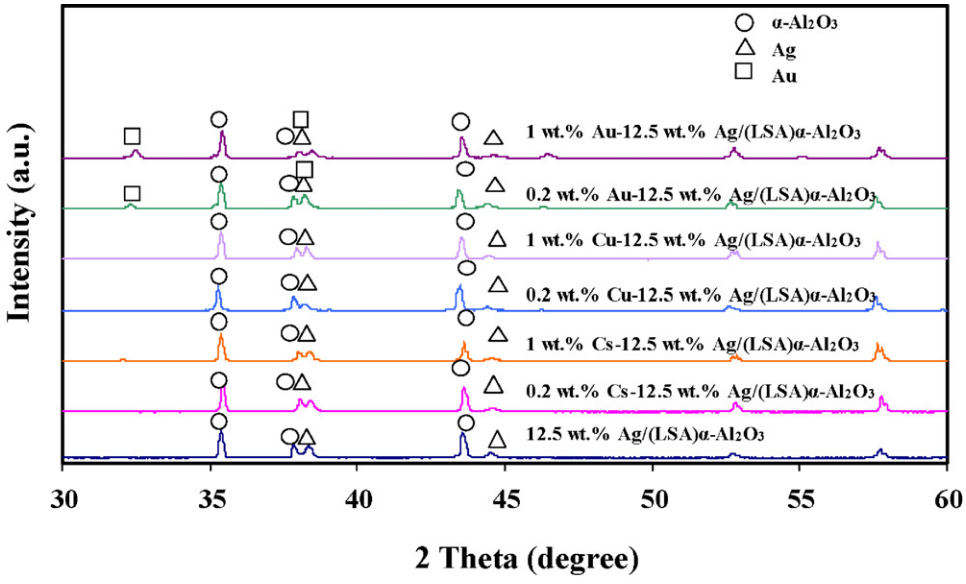

Fig. 2. XRD patterns of all investigated catalysts.

All the product selectivities, except H_2 selectivity, are calculated based on the numbers of C atom in C_2H_4 and product, and moles of C_2H_4 converted and product produced.

The EO yield is calculated from the following equation:

$$\%\text{EO yield} = \frac{(\%\ C_2H_4\text{conversion})\,(\%\text{EO selectivity})}{(100)}$$

To determine the energy efficiency of each plasma system, the specific power consumption is calculated in a unit of Ws per molecule of converted C_2H_4 or per molecule of produced EO using the following equation:

$$\text{specific power consumption} = \frac{(P)(60)}{(N)(M)}$$

where P, Power (W); N, Avogadro's number = 6.02×10^{23} molecules/mol, and M, rate of converted C_2H_4 molecules in the feed or the rate of produced EO molecules (mol/min).

Table 1
Specific surface area and amount of coke formed for all investigated catalysts used for the corona discharge system.

Catalyst	Specific surface area (m^2/g)	Coke formation (%)
12.5 wt.% Ag/(LSA)α-Al_2O_3	0.28	0.26
0.2 wt.% Cs–12.5 wt.% Ag/(LSA)α-Al_2O_3	0.33	0.11
1 wt.% Cs–12.5 wt.% Ag/(LSA)α-Al_2O_3	0.44	0.16
0.2 wt.% Cu–12.5 wt.% Ag/(LSA)α-Al_2O_3	0.39	0.14
1 wt.% Cu–12.5 wt.% Ag/(LSA)α-Al_2O_3	0.74	0.22
0.2 wt.% Au–12.5 wt.% Ag/(LSA)α-Al_2O_3	0.33	0.75
1 wt.% Au–12.5 wt.% Ag/(LSA)α-Al_2O_3	0.42	1.07

3. Results and discussion

In this work, four types of catalysts – Ag/(LSA)α-Al_2O_3, Cs–Ag/(LSA)α-Al_2O_3, Cu–Ag/(LSA)α-Al_2O_3, and Au–Ag/(LSA)α-Al_2O_3 – were used for investigating the ethylene epoxidation activity in the combined catalytic and corona discharge system.

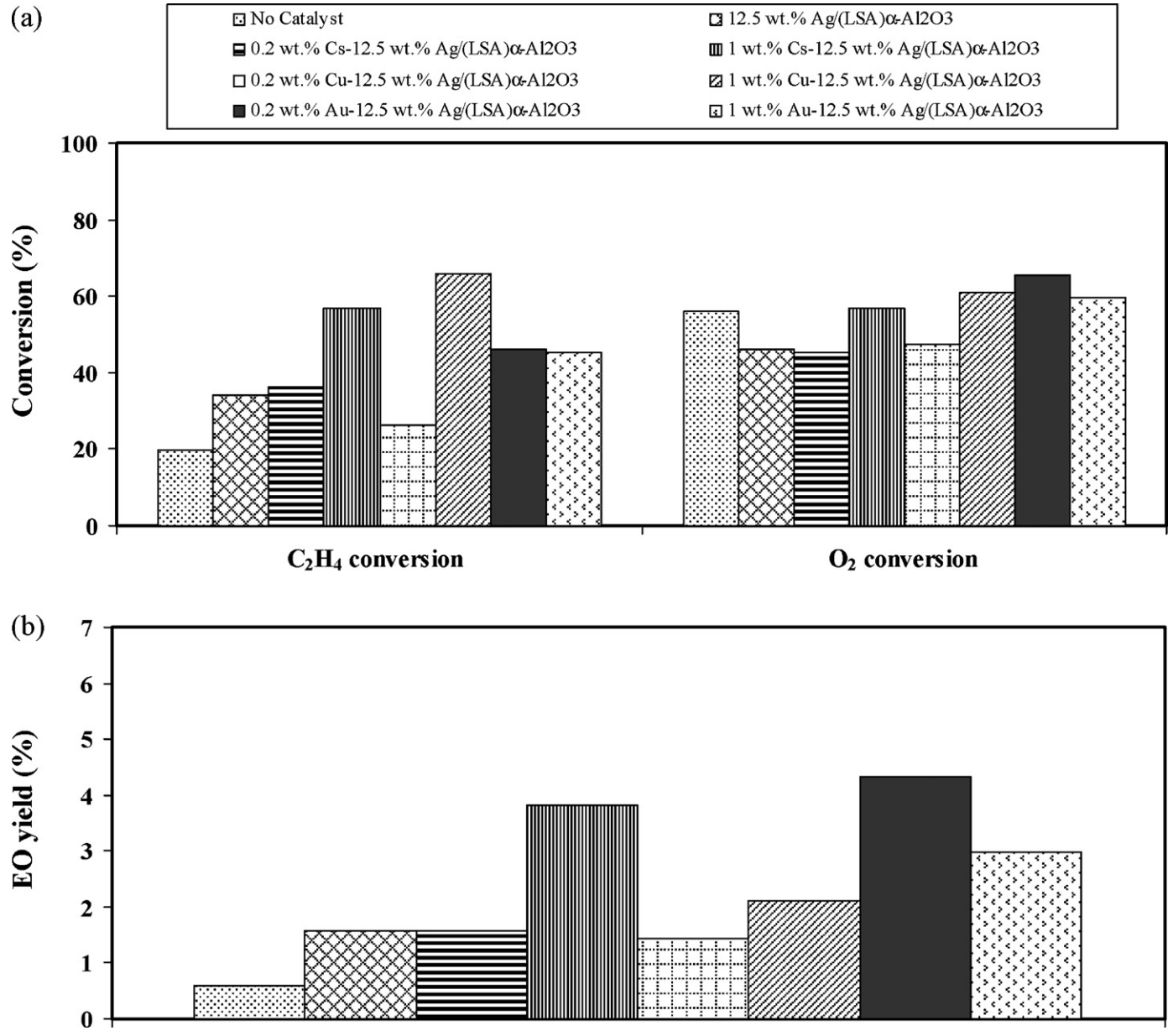

Fig. 3. Comparison of (a) C_2H_4 and O_2 conversions and (b) EO yield of the corona discharge system over Ag catalyst with different promoters.

The specific surface areas of all investigated Ag/(LSA)α-Al_2O_3-based catalysts are shown in Table 1. The results indicate that when the three, second metals (Cs, Cu, and Au) were sequentially loaded on the Ag/(LSA)α-Al_2O_3 catalyst, the specific surface areas of all bimetallic catalysts slightly increased. This implies that all the loaded second metals showed good dispersion on the Ag/(LSA)α-Al_2O_3 catalyst. Because of the insignificantly different specific surface areas of all the catalysts, it can be hypothesized that the specific surface area plays a less significant role than the property of the metals themselves on the epoxidation activity.

XRD patterns of all the studied catalysts were obtained (Fig. 2), and all of the bimetallic catalysts show the same XRD patterns as the monometallic Ag/(LSA)α-Al_2O_3 catalyst, mainly consisting of α-Al_2O_3 and Ag phases. For the Au–Ag/(LSA)α-Al_2O_3 catalyst, the peaks corresponding to the Au phase were clearly observed. For both the Cs–Ag/(LSA)α-Al_2O_3 and the Cu–Ag/(LSA)α-Al_2O_3 catalysts, however, there was no clear evidence of any peaks corresponding to Cs and Cu. This is possibly due to their light mass as compared to that of Au at the same wt.% loadings.

Under the plasma environment, the gas phase reactions induced by the discharge mainly contribute to the reactant conversions. In the corona discharge system used in this work, most of the discharge energy is used to produce and accelerate electrons, which instantaneously react with gas molecules (C_2H_4 and O_2) to generate several highly active species (metastable radicals and ions) [26]. It was experimentally found that the C_2H_4 and O_2 conversions and the EO yield were significantly enhanced by using all the bimetallic catalysts with a suitable second metal loading, as compared to the monometallic Ag catalyst and the system without catalyst (Fig. 3). Among the investigated catalysts, the 1 wt.% Cs–12.5 wt.%

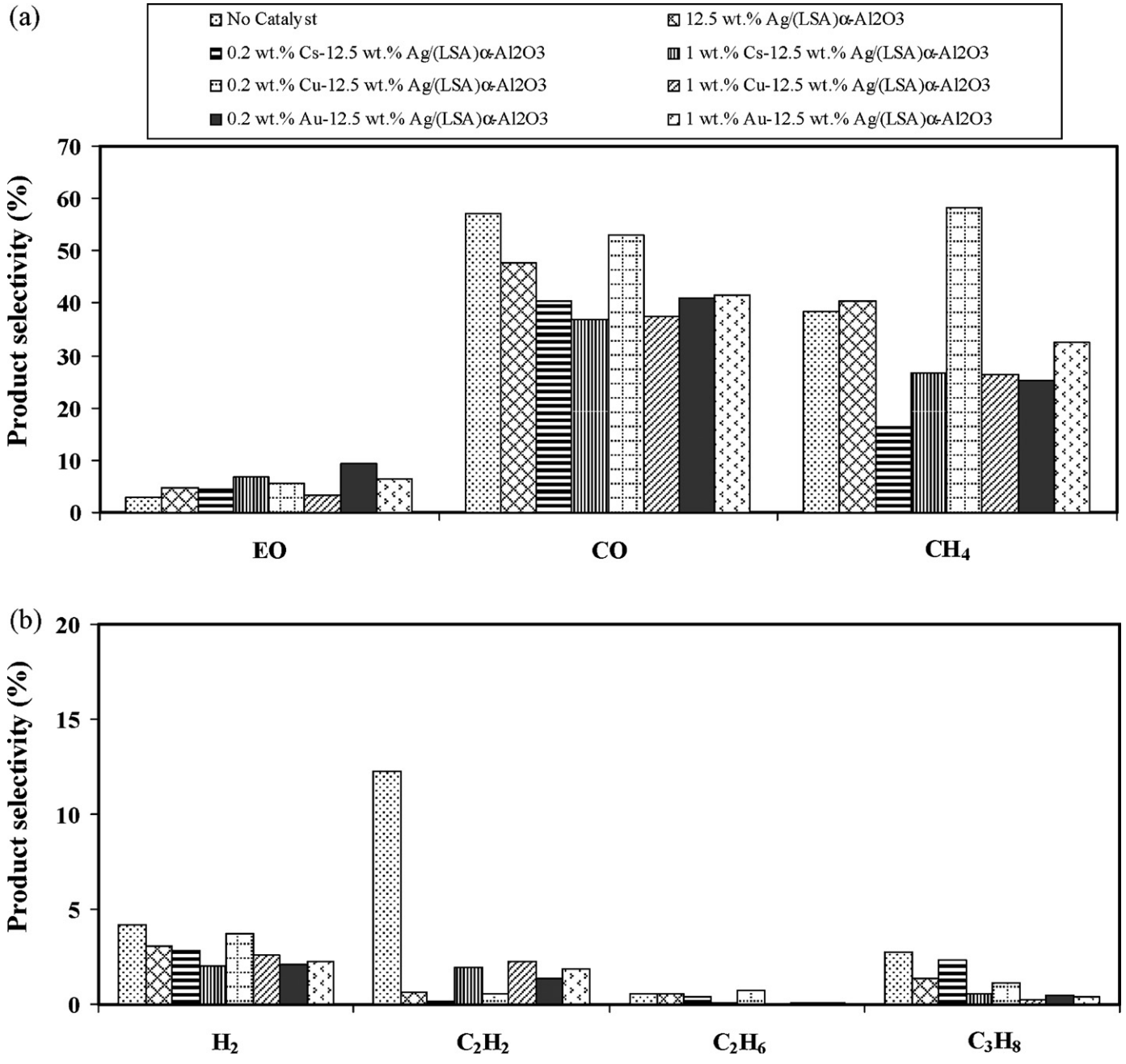

Fig. 4. Comparison of product selectivities for (a) EO, CO, and CH_4, and (b) H_2, C_2H_2, C_2H_6, and C_3H_8 of the corona discharge system over Ag catalyst with different promoters.

Ag/(LSA)α-Al_2O_3 and the 0.2 wt.% Au–12.5 wt.% Ag/(LSA)α-Al_2O_3 catalysts provided a comparatively high EO yield. The use of Cu as the promoter, however, slightly increased the EO yield only at the high loading of 1 wt.%, while 0.2 wt.% Cu showed no improvement of the EO yield as compared to the monometallic Ag catalyst.

The main products of the studied plasma system with different bimetallic catalysts were EO, CO, CH_4, and H_2 with trace amounts of C_2H_2, C_2H_6, and C_3H_8 (Fig. 4). No CO_2 was observed from ethylene epoxidation in the studied corona discharge system. It can be seen that the type of catalysts significantly affected the selectivities for the main products. Particularly, the bimetallic 1 wt.% Cs–12.5 wt.% Ag/(LSA)α-Al_2O_3 and the 0.2 wt.% Au–12.5 wt.% Ag/(LSA)α-Al_2O_3 catalysts combined with plasma were found to be favorable for the ethylene epoxidation reaction, compared to the other catalysts. Moreover, they provided a relatively low amount of CO, as well as low selectivities for H_2, C_2 products, and C_3H_8. From the results, it can be concluded that for the sole corona discharge system, both the EO selectivity and yield were relatively low because most reactions occur in the gas phase, and C_2H_4 is mostly split into CH_4 and is partially oxidized to CO. In the presence of the monometallic Ag catalyst, the C_2H_4 conversion and both the EO selectivity and yield greatly increased, compared to the sole corona discharge system; this is because the system provided the additional Ag active sites for molecular oxygen adsorption to consequently favor ethylene epoxidation [28]. The Cs promoter added on the Ag catalyst, moreover, neutralizes acid sites on the catalyst surface, which are active for the further isomerization and oxidation of EO [29], and adjusts the surface electron density to reduce the binding strength of EO to the catalyst surface, resulting in less oxidized product formation [30]. In addition, Cs plays a role in increasing the adsorption probability of oxygen on the Ag active sites [31]; whereas, the Au promoter affects the electronic properties of Ag by weakening the Ag–O bond strength, which, in turn, promotes ethylene epoxidation [19,28]. It was experimentally found that in the presence of small amounts of Au (lower than 0.54 wt.%) on the Ag catalyst, the interaction between the Au and Ag significantly enhanced the oxygen adsorption for the ethylene epoxidation; however, a higher Au addition (greater than 0.54 wt.%) caused the Au–Ag alloy formation, instead of Au–Ag bimetallic formation, which was proved to be disadvantageous for ethylene epoxidation [28]. It can also be seen from the present work, using the combined catalytic–corona discharge system, that a low Au addition of 0.2 wt.% showed much better epoxidation performance than a high Au addition of 1 wt.%, probably by a consequence of the Au–Ag bimetallic formation as aforementioned. In other words, when the Au addition increased from 0.2 (small amount) to 1 wt.% (sufficiently large amount), it can possibly form alloy with Ag (12.5 wt.%). This Au–Ag alloy formation negatively affected the epoxidation performance. Therefore, a suitable addition of each promoter should be used.

In general observation, it was found that the power consumptions per EO molecule produced and per C_2H_4 molecule converted were greatly reduced in the presence of all the studied catalysts (Fig. 5). The power consumption per EO molecule produced was much higher than that per C_2H_4 molecule converted. For a comparison among the promoters, both Cs and Au added on the Ag catalyst significantly helped reduce the power consumption per EO molecule produced, and the lowest power consumption per EO molecule produced was found with the 1 wt.% Cs–12.5 wt.% Ag/(LSA)α-Al_2O_3 and the 0.2 wt.% Au–12.5 wt.% Ag/(LSA)α-Al_2O_3 catalysts, which exhibited good epoxidation performance (Figs. 3 and 4).

After the plasma reaction testing experiments, the spent catalysts were analyzed to determine the amount of coke deposited on the catalyst surface (Table 1), and the Ag partcle size. It can be clearly seen in the table that there were, overall, extremely low amounts of coke formed on all the studied catalysts. However, the Au–Ag/(LSA)α-Al_2O_3 catalysts, which exhibited the comparatively good epoxidation performance, tended to induce slightly higher coke formation. TEM was employed to observe the mean particle size of the Ag nanoparticles on the surface of the investigated catalysts (Fig. 6). The results from the high resolution TEM (HRTEM) analysis show that Ag nanoparticles are highly dispersed on the alumina support for the freshly prepared catalysts. As exempli-

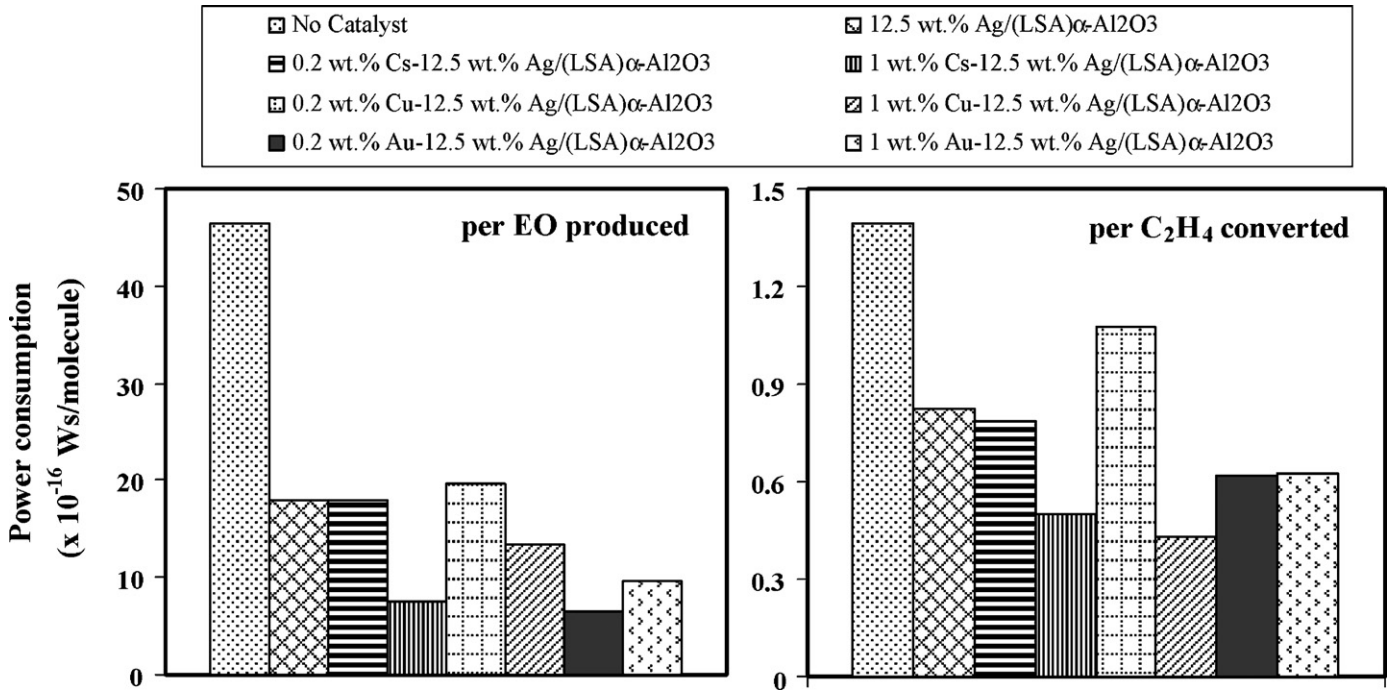

Fig. 5. Comparison of power consumptions per EO molecule produced and per C_2H_4 molecule converted of the corona discharge system over Ag catalyst with different promoters.

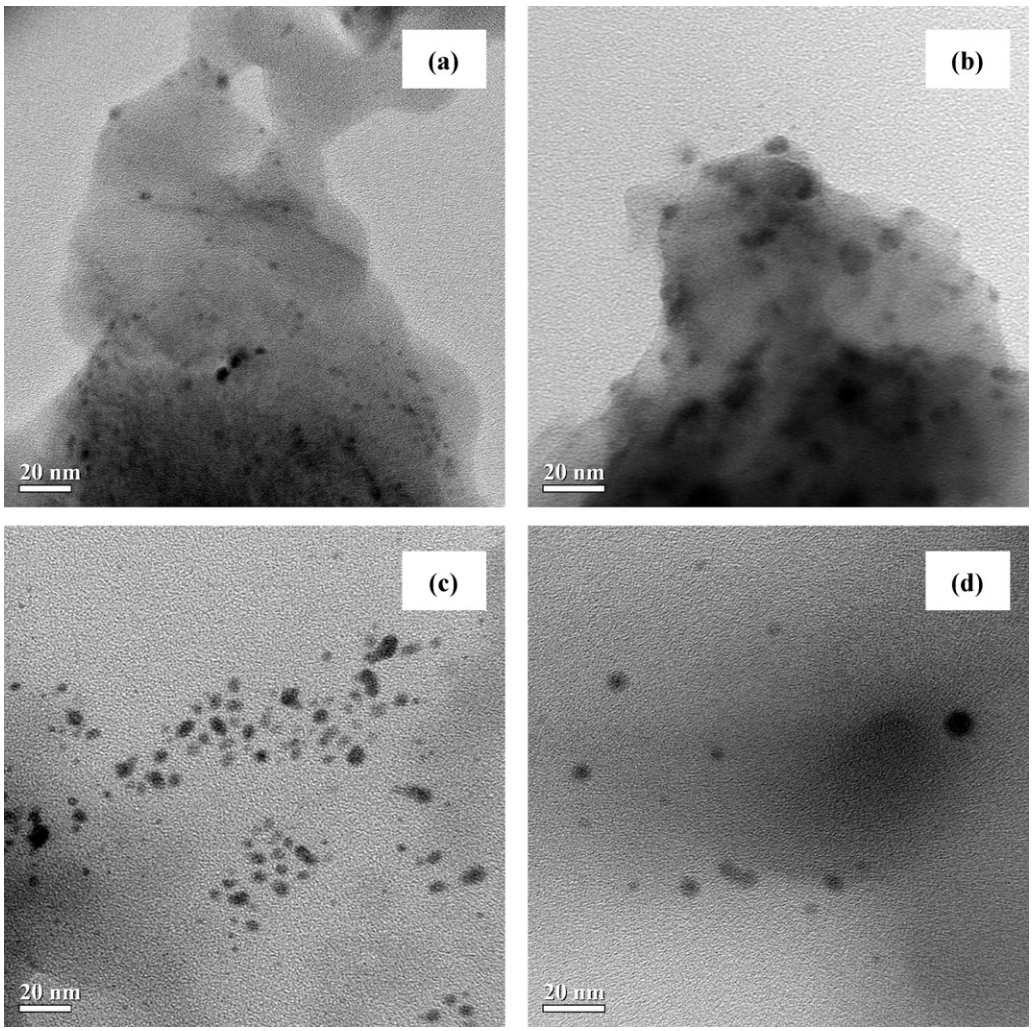

Fig. 6. HRTEM micrographs of Ag nanoparticles on (a) fresh and (b) spent 1 wt.% Cs–12.5 wt.% Ag/(LSA)α–Al_2O_3 catalyst, and (c) fresh and (d) spent 0.2 wt.% Au–12.5 wt.% Ag/(LSA)α-Al_2O_3 catalyst.

fied in Fig. 6, the HRTEM micrographs of the 1 wt.% Cs–12.5 wt.% Ag/(LSA)α-Al_2O_3 and the 0.2 wt.% Au–12.5 wt.% Ag/(LSA)α-Al_2O_3 catalysts, which exhibited superior activity toward ethylene epoxidation, as explained above, show average Ag particle sizes of approximately 5–7 nm for both of the fresh catalysts and approximately 9–12 nm for both of the spent catalysts, suggesting that the Ag agglomeration occurred after the activity testing under the corona discharge environment. This Ag agglomeration on the surface of the spent catalysts possibly results from the high energy intensity from the corona discharge with the pin and plate electrodes used in this work. For the corona discharge used in this work, the bulk gas temperature is comparatively low; however, the energetic electrons may have energy ranging from 1 to 10 eV, corresponding to extremely high temperatures of about 10^4–10^5 K [23–25]. This intense electron collision can induce a significant increase in the temperature of a number of micro-sized spots on the whole catalyst surface, inevitably leading to the Ag agglomeration. Even though the Ag agglomeration occurs on the catalyst surface, the Ag particle sizes are still very tiny, in the nanometer range (below 15 nm), and the Ag nanoparticles are still highly dispersed on the alumina support. To solve this Ag agglomeration, an ongoing research is being conducted with other types of plasma reactors, such as DBD, in our group. If this problem is resolved, the durability of the catalyst is also necessary to be investigated in our future work.

4. Conclusions

In this work, ethylene epoxidation was investigated in a combined catalytic–corona discharge system. The catalysts used were (LSA)α-Al_2O_3-supported 12.5 wt.% Ag with a 0.2 or 1 wt.% Cs, Cu, or Au promoter. The addition of the promoter on the Ag catalyst helps enhance the ethylene conversion and the EO yield and selectivity when combined with the corona discharge, especially for the 1 wt.% Cs–12.5 wt.% Ag/(LSA)α-Al_2O_3 and the 0.2 wt.% Au–12.5 wt.% Ag/(LSA)α-Al_2O_3 catalysts. The corona discharge system, combined with these catalysts, also consumed relatively low power to produce the EO molecule.

Acknowledgements

The authors would like to thank the Ratchadapisek Somphot Endowment Fund, Chulalongkorn University, Thailand; the Sustainable Petroleum and Petrochemicals Research Unit, Center for Petroleum, Petrochemicals, and Advanced Materials, Chulalongkorn University, Thailand; and the Petrochemical and Environmental Catalysis Research Unit under the Ratchadapisek Somphot Endowment Fund, Chulalongkorn University, Thailand.

References

[1] P.P. McClellan, Ind. Eng. Chem. 42 (1950) 2402.

[2] S. Matar, M.J. Mirbach, H.A. Tayim, Catalysis in Petrochemical Processes, Kluwer Academic Publishers, Dordrecht, The Netherlands, 1989.
[3] J.G. Serafin, A.C. Liu, S.R. Seyedmonir, J. Mol. Catal. A: Chem. 131 (1998) 157.
[4] K.L. Yeung, A. Gavriilidis, A. Varma, M.M. Bhasin, J. Catal. 174 (1998) 1.
[5] W.S. Epling, G.B. Hoflund, D.M. Minahan, J. Catal. 171 (1970) 490.
[6] S.N. Goncharova, E.A. Paukshtis, B.S. Bal'zhinimaev, Appl. Catal. A: Gen. 126 (1995) 67.
[7] M.A. Peña, D.M. Carr, K.L. Yeung, A. Varma, Chem. Eng. Sci. 53 (1998) 3821.
[8] D. Lafarga, A. Varma, Chem. Eng. Sci. 55 (2000) 749.
[9] E.A. Podgornov, I.P. Prosvirin, V.I. Bukhtiyarov, J. Mol. Catal. A: Chem. 158 (2000) 337.
[10] A. Ayame, Y. Uchida, H. Ono, M. Miyamoto, T. Sato, H. Hayasaka, Appl. Catal. A: Gen. 244 (2003) 59.
[11] M.C.N. Amorim de Carvalho, F.B. Passos, M. Schmal, J. Catal. 248 (2007) 124.
[12] S. Linic, J. Jankowiak, M.A. Barteau, J. Catal. 224 (2004) 489.
[13] J.T. Jankowiak, M.A. Barteau, J. Catal. 236 (2005) 366.
[14] J.T. Jankowiak, M.A. Barteau, J. Catal. 236 (2005) 379.
[15] J.C. Dellamorte, J. Lauterbach, M.A. Barteau, Catal. Today 120 (2007) 182.
[16] P.V. Geenen, H.J. Boss, G.T. Pott, J. Catal. 77 (1982) 499.
[17] N. Toreis, X.E. Verykios, J. Catal. 108 (1987) 161.
[18] R. Herrera, A. Varma, E. Martínez, Stud. Surf. Sci. Catal. 55 (1990) 717.
[19] D.I. Kondarides, X.E. Verykios, J. Catal. 158 (1996) 363.
[20] S. Rojluechai, S. Chavadej, J.W. Schwank, V. Meeyoo, Catal. Commun. 8 (2007) 57.
[21] S. Chavadej, S. Rojluechai, J.W. Schwank, V. Meeyoo, Mechanisms in Homogeneous and Heterogeneous Epoxidation Catalysis, Elsevier, 2008, p. 283.
[22] B. Elissson, U. Kogelschatz, IEEE Trans. Plasma Sci. 19 (1991) 1063.
[23] H. Suhr, H. Pfreundschuh, Plasma Chem. Plasma Process. 8 (1988) 67.
[24] L.A. Rosacha, G.K. Anderson, L.A. Bechtold, J.J. Coogan, H.G. Heck, M. Kang, W.H. McCulla, R.A. Tennant, P.J. Wantuck, NATO ASI Ser. Part B (1993) 34.
[25] P. Patiño, F.E. Hernández, S. Rondón, Plasma Chem. Plasma Process. 15 (1995) 159.
[26] S. Chavadej, A. Tansuwan, T. Sreethawong, Plasma Chem. Plasma Process. 28 (2008) 643.
[27] T. Sreethawong, T. Suwannabart, S. Chavadej, Plasma Chem. Plasma Process. 28 (2008) 629.
[28] S. Rojluechai, S. Chavadej, J.W. Schwank, V. Meeyoo, J. Chem. Eng. Jpn. 39 (2006) 321.
[29] W.S. Epling, G.B. Hoflund, D.M. Minahan, J. Catal. 171 (1997) 490.
[30] S.A. Tan, R.B. Grant, R.M. Lambert, J. Catal. 106 (1987) 54.
[31] M. Kitson, R.M. Lambert, Surf. Sci. 109 (1981) 60.